A Simple and Rapid Evaluation of Explosive Performance – The Disc Acceleration Experiment

Karl Thomas Lorenz, Edward L. Lee and Ronald Chambers

June 03, 2014

A SIMPLE AND RAPID EVALUATION OF EXPLOSIVE PERFORMANCE – THE DISC ACCELERATION EXPERIMENT

Karl Thomas Lorenz, Edward L. Lee, and Ronald Chambers
Energetic Materials Center
Lawrence Livermore National Laboratory
Livermore, CA

ABSTRACT

It is crucial in the development of a new explosive to obtain an evaluation of performance early in the process when the availability of material is limited. Evaluation requires dynamic measurements of detonation velocity, pressure, and expansion energy - typically in separate experiments that require large amounts of material, time, and expense. There is also a need for evaluation of the total available thermodynamic energy. The dynamic evaluations, in particular, have been a major hindrance to development of new explosives. The new experimental testing method to be described here requires small charges and obtains accurate measurement of all three of the detonation performance characteristics in a single test. The design, a Disc Acceleration eXperiment (DAX), provides an initial condition of steady detonation and a charge-geometry amenable to 2D hydrodynamic simulations. The velocity history of a metal disk attached to the end of the explosive charge is measured with Photonic Doppler Velocimetry (PDV). This disc velocity data is analyzed to give both CJ pressure and expansion energy. The detonation velocity is obtained with probes along the charge length. The experiments and subsequent analyses are concentrated on LX-16, a known PETN based explosive, for the purpose of establishing the accuracy of the method and to provide a standard for comparison with other explosives. We will present details of the experimental design and also detonation velocity and PDV results from a number of experiments. The total available internal energy for the explosive was obtained from published detonation calorimetry measurements by Ornellas [1], and from thermodynamic equilibrium calculations. An equation-of-state (EOS) for LX-16 was derived from hydrodynamic simulations of thin plate-push velocity-time data. We will show a successful comparison with a previously published Jones-Wilkins-Lee (JWL) EOS for PETN by Green & Lee [2-4].

INTRODUCTION

There are a great many experimental tests that have been used to determine the performance of new explosives. Besides standard rate sticks, which are used to measure the detonation-front velocities of explosives, Cooper lists six of the most commonly used test configurations for determining the energy, or power, of an explosive: the sand test, ballistic mortar test, Trauzl test, plate dent test, fragmentation test and cylinder test [5]. Most of these are static recovery tests that measure the integrated load on a witness material. The greater the load - as measured by the size of the movement of witness material, the greater the energy content in the explosive and the pressure imposed by the detonation front. The cylinder test, on the other hand, is a dynamic test in that it measures the velocity of a copper witness tube as it enlarges radially in time with the expanding detonation product gases. The energy of the cylinder walls is directly related to the square of the measured wall velocity history and is assumed to be proportional to the energy of the expanding product gases. Using high-speed cameras or laser velocimetry, the wall energy (and product gas energy) can be measured as a function of product gas volume. From this data an equation-of-state can be derived for the explosive. This technique has matured enough to serve as the standard method for determining JWL EOS's for new explosives [6-9]. The classic analysis iteratively adjusted the JWL parameters to match the experimental wall energies at the defined relative volumes of the product gases. The gas volumes are straightforward to calculate based on the wall displacements (directly from streak camera measurements, or determined by numerical integration of the velocity-time data). Modern cylinder tests provide excellent data for product gas volume expansion ratios as large as ~10 [10]. The addition of laser velocimetry has made the initial expansion region that is most sensitive to the Chapman-Jouget (CJ) state easier to analyze with higher precision. However, the current methods for

extracting the JWL EOS from the wall energies still treat the important performance parameter - CJ pressure, as an adjustable parameter in the JWL EOS. Modern fitting algorithms using minimization techniques can rapidly develop a full JWL beginning with the density, detonation velocity, and the cylinder wall energies at 2 or 3 relative gas volumes [10]. With enough resources, an independent measurement of the CJ-state can be undertaken. Plate-push measurements have been obtained from experiments using thicker witness plates, and charge geometries that stressed detonation front planarity [11-13]. Other overdriven methods have also been used to investigate the CJ state of common explosives [14]. However, many of these experiments would entail large costs in today's R&D environment, which can be a barrier in the early stages of developing a new explosive.

The current LLNL cylinder test uses photonic Doppler velocimetry [15], or PDV, diagnostics to track the wall velocity at multiple points around and along the cylinder. This has resulted in very high precision data, but also relatively high shot costs. In addition to the costs of precision cylinders and multiple diagnostics, a standard 25.4mm diameter cylinder test also requires as much as 250g of sample material. Despite the high fidelity of this test, the resources required make this test unsuitable for performance testing of newly synthesized explosives, where the total amount of available material may be only 10's of grams. In response to this need, we have begun development on a high-precision performance test that will deliver data on a variety of performance metrics, but using minimal resources. The experimental assembly is a basic small-scale rate stick (using less than 20 grams of sample material), but includes a thin witness plate (or disc) at the end of the rate stick. Using a combination of timing pins and one laser velocimetry probe, this Disc Acceleration eXperiment, or DAX, generates data for extracting detonation velocity, CJ-pressure and detonation energy (at relative volume expansions of 2-3). Considering development costs to date, we estimate the total cost reductions of ~10x over traditional cylinder experiments. This includes formulation, pressing, machining, shot assembly, firing facility costs, and post-shot analysis. These costs are expected to hold or even decrease as the DAX design becomes standardized. The experimental method described in this report yields all of the required experimental results for a chosen explosive in each test shot. We will describe the test configuration and methods, and will also details on how the velocity-time data can be used to determine the CJ state with high accuracy.

EXPERIMENTAL

Figure 1 shows a schematic of the basic design of the DAX assembly - showing only the most essential features. The image on the right shows a pair of completed assemblies waiting to be placed into the firing tank. The DAX assembly consists of 12.7mm diameter pellets (either three 25.4mm long or six 12.7mm long) stacked end to end for a total sample length of ~75mm. With the addition of a PBX-9407 booster (94% RDX, 6% VCTFE), most new and existing explosives obtain steady-state propagation well before the front reaches the end of the rate stick. At that point, the detonation products expand and accelerate a thin metal disc, which is tracked using Photonic Doppler Velocimetry (PDV). These witness discs are either 425-μm thick aluminum (1100 series alloy) or 250- μm thick copper (CDA 110, soft). The acrylic (PMMA) sleeve that surrounds the explosive pellets holds the PDV probe on the geometric axis at a position 10 cm from the thin metal witness disc. These tubes are precision machined from rod stock, which allows for close tolerance fits of all the parts. The positions for the piezoelectric timing pins are known to better than ±50μm, which contributes to the precision of the detonation velocity measurement. The PDV diagnostic measures the accelerating witness plate, which serves as the primary metric of explosive performance for DAX. A detailed analysis of the plate velocity allows us to make accurate estimates of CJ pressure, product gas energies and JWL EOS's. This will be discussed in detail below. PDV is a technique that was developed at LLNL [15]. The PDV technique has exceptionally high precision, and requires a minimum of equipment. Standard piezoelectric timing pins [16] are used to track the detonation velocity. Multiple assemblies can be fired simultaneously, which substantially reduces facility costs. This requires sufficient data collection channels for the timing pins. By using a summing box, the signals from each of the six timing pins for any given DAX assembly can be input into a single digitizer channel. We currently fire four shot assemblies at a time, which contributes to the overall cost efficiencies of this experimental design.
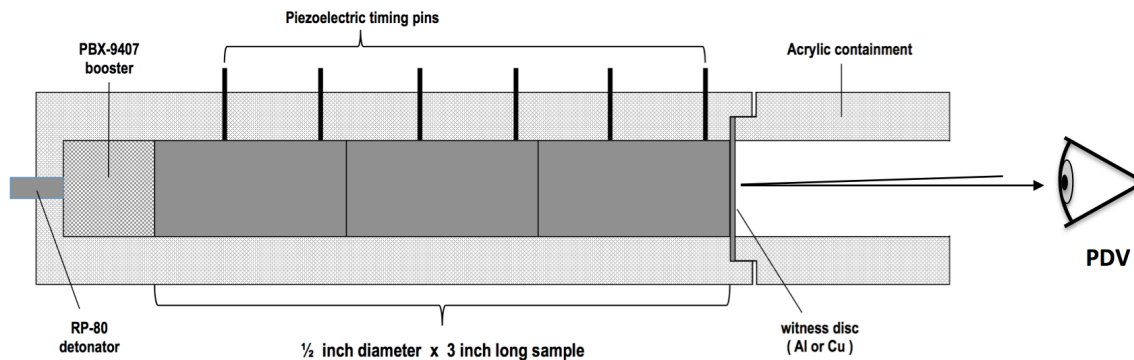
Figure 1: Schematic of the Disc Acceleration Experiment, or DAX. This design uses less than 20 grams of sample material and obtains better than 1% precision on $V/V_0 \sim 2\text{-}3$ energy output. Detonation velocities are extracted with estimated uncertainties of 0.2-0.4%. The PDV velocity-probe that tracks the witness foil acceleration is fixed to the end of a 100mm long acrylic extension and fiber coupled to the PDV detection hardware. A series of 6 piezoelectric pins track detonation velocity. Multiple probes can be connected to the PDV system, allowing us to fire as many as four DAX assemblies at one time.

PETN has long been considered as a standard of measure for explosive performance, partly due to its near-ideal detonation behavior. The oxygen balance is very good (-10%), and the detonation kinetics are not generally constrained by normal charge sizes or environmental conditions, such as temperature. Therefore, PETN serves as an excellent calibration standard for any new detonation performance test. LX-16 is a well-established and tested DOE explosive formulation consisting of 96.5 weight percent PETN and 3.5 weight percent binder (VCTFE, or a mixture of the monomers vinyl chloride and trifluoroethylene). The addition of a binder facilitates the pressing of the LX-16 molding powder into uniformly dense pellets. Density variations in the explosive pellets are a primary source of issues in shot-to-shot repeatability, and must be kept to a minimum. DAX assemblies were built using both aluminum (425-µm thick) and copper (254-µm thick) witness discs. Table 1 lists the details for the six assemblies that were tested for this study.

Table 1: shows the details for the six DAX shots that were fired for calibrating this new technique using LX-16. The table lists the shot identification, witness disc material and thickness, average pellet density (measured by mass and dimensional volume), and the measured detonation velocity. The details for the detonation velocity measurements follow below.

Shot ID	Witness Metal	Disc Thickness (mm)	Pellet Density (g/cc)	Detonation Velocity (mm/µs)	ΔD_V (Std. Dev., %)
TLX-XII-048	copper	0.254 ± 0.010	1.730	8.150	0.094
TLX-XII-049	copper	0.254 ± 0.010	1.732	8.140	0.111
TLX-XII-050	copper	0.254 ± 0.010	1.734	8.162	0.064
TLX-XII-051	aluminum	0.425 ± 0.015	1.734	8.164	0.084
TLX-XII-052	aluminum	0.425 ± 0.015	1.736	8.151	0.314
TLX-XII-053	aluminum	0.425 ± 0.015	1.738	No Data	N/A

The reason for using both copper and aluminum discs was to explore any measurement/performance sensitivity to the metal mass, and to test the generality of our methodology for extracting CJ pressures from the DAX velocity-time data. The measurement of the CJ pressure of an explosive formulation is difficult and normally beset with large uncertainties, or it must be inferred indirectly from the experimental

data. However, the CJ pressure for PETN has been examined in detail and has been well established as a function of pellet density [4]. In addition to the measurement of the critical parameters of detonation velocity and CJ pressure, Green & Lee also recently published a refined JWL EOS [3] for PETN based on previous work [2]. Finally, the initiation characteristics of LX-16 have been studied and published by Tarver and May [17]. These authors published an EOS for LX-16 that we could use for comparison purposes. However, their experiments were designed to study initiation thresholds and subsequent growth to detonation. Therefore, we have chosen to use the PETN studies of Green and Lee describing steady detonation. The Green & Lee JWL is a "near-neighbor" formulation that will serve as a comparison to the EOS we develop for LX-16 using the new DAX methodology.

Timing pin data is acquired and treated in the standard way for extracting detonation velocities. The times for the pin signals are plotted against the pin positions and fit to a linear function. The slope of the fitted line is reported as the detonation velocity. The last column in Table 1 shows the standard deviation (expressed as a percent of the detonation velocity) for the fit to the distance-time data. The uncertainty in the fit is well below 0.5%. Figure 2 shows a representative plot of the voltage traces from a set of timing pins, as well as a fitted line to the position-time data. This set of data is from shot TLX-XII-052 (see Table 1 above). The timing pins cover most of the 75mm of sample material, at 12.7mm intervals. We generally see very little change in the velocity over that sample distance. For non-ideal explosives, steady-state behavior may require longer run distances. However, this data – which does not include the region with the PBX 9407 booster, indicates steady detonation for the entire range of measurement. Note that the pins technically are measuring the phase velocity of the detonation front at the edge of the charge. However, for steady detonation, this phase velocity is equal to the centerline detonation velocity.
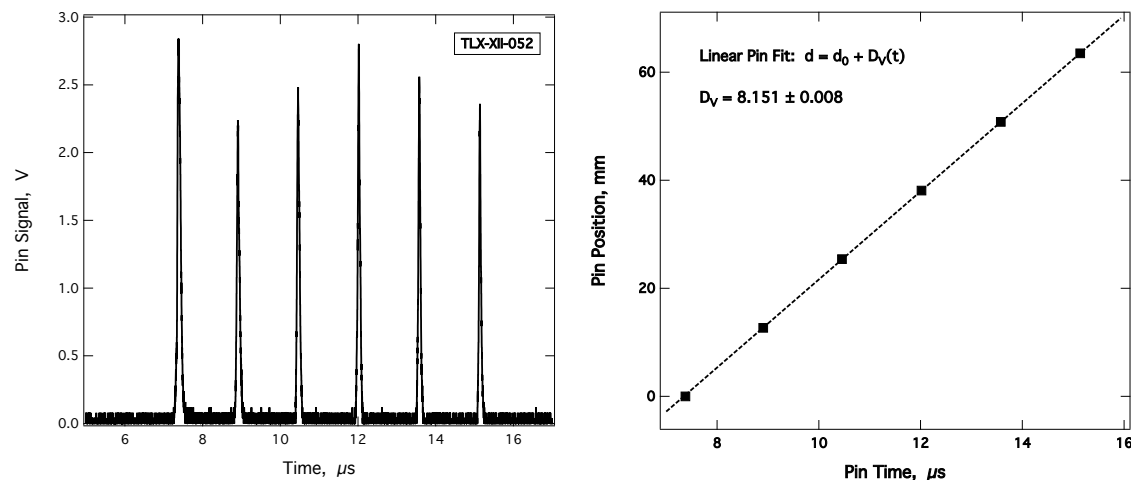

Figure 2: Piezoelectric timing pin data and detonation-velocity analysis. The signal traces for six timing pins are shown in the plot on the left. Times are taken from the peaks of the individual voltage profiles. These time values are then plotted against the positions of the precision-machined hole for the pins. The data is fit to a linear function, and the slope of the line is a measure of the detonation velocity.

The core performance metric for the DAX technique is the time-dependent behavior of the thin metal witness discs that are placed at end of the charge column. The launch, and subsequent acceleration, of the witness disc is tracked using Photonic Doppler Velocimetry, or PDV [15]. The energy of the expanding product gases is reflected in the trajectory of the accelerating disc. Aziz has made estimates of coupling efficiencies to the witness plate for a one-dimensional idealized case [18]. The amount of energy coupled to a witness plate depends on the relative masses of the explosive and witness plate. The maximum coupling converts about 35% of the available detonation energy for this geometry into kinetic energy of the witness plate. Peak coupling occurs for an explosive-to-plate mass ratio of 2-3. For our configuration, the mass of explosive is poorly defined. Gurney analyses suggest that the participating explosive mass consists of a 60-degree cone of material behind the plate [18, 19]. Assuming a 60-degree cone, and using

our 0.425-mm thick aluminum plate, our explosive-plate mass ratio is about 14 – suggesting a coupling efficiency of 20%. For the 0.254-mm copper case, the explosive-mass ratio is halved to about 7, which pushes the theoretical coupling efficiency up to about 30%. Figure 3 shows the disc trajectory (velocity versus time) data for a single DAX shot (Shot number TLX-XII-050). The initial motion of the foil's rear surface (away from the sample) is a free surface "jump-off velocity" that is approximately twice the in-material particle velocity. An analysis of this jump-off region is used to extract the CJ-pressure, as will be explained below. The disc continues to accelerate in steps, due to the reverberating pressure wave inside the disc. This is a common condition for foils and thin plates driven by explosives. The time-dependent pressure wave (Taylor wave) behind the detonation front results in a series of compression and release waves in the disc, which are observed as accelerations and decelerations of the back surface of the witness disc. A generalized position-time description of the reverberating waves is shown in Fig. 3 in the right-hand schematic [20].
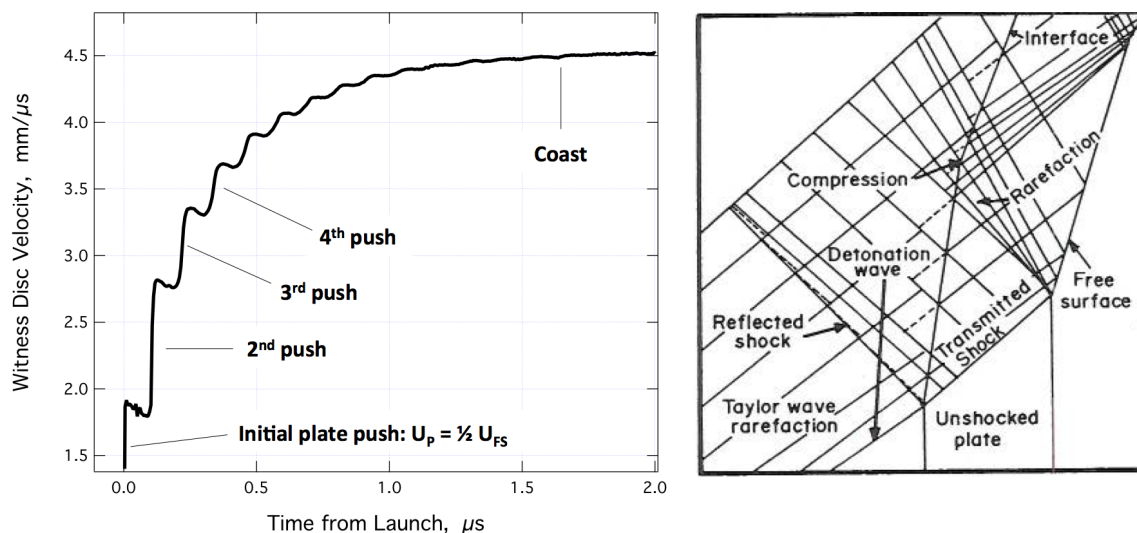

Figure 3: Velocimetry data for a 254μm Cu witness foil accelerated by LX-16 detonation products. The velocity oscillations are the standard signature for the compression-release waves that move back and forth in a thin foil driven by a Taylor wave. The diagram on the right depicts the position-time trajectories for the compression and release waves. Time is on the vertical axis, and position is on the horizontal axis [20]. Note that the description based on the method of characteristics in the right hand figure does not include material strength.

RESULTS

The measured disc trajectories correlate with the energy of the expanding product gases. The disc velocities can be used to determine the energy release of the explosive much as one does with the wall velocities in the cylinder test [7-9]. As stated above, the fraction of available energy in the detonation products that couples to kinetic energy in the witness material is dependent upon the experimental geometry and relative masses of explosive and witness material. However, in any given experimental geometry we generally assume that the fraction of detonation energy coupled to witness motion is constant across all explosives. This assumption allows us to correlate the witness-disc energy to detonation energy in the explosive and to make relative rankings of energy release in different explosives. Figure 4 shows velocity-time profiles of the accelerating witness disc for LX-16 using two different witness disc materials and thicknesses. Three traces are shown for each of the two configurations. The shot-to-shot repeatability over the entire time domain of the disc's trajectory is excellent. The region having largest velocity spread is shown in the figure to have a standard deviation of ±0.75%. This corresponds to an energy spread of ~1.5% within a small region of the overall data record. In the "coast" region (around 2 μs), the copper disc has 33% more kinetic energy than the aluminum disc. This indicates the improved

coupling efficiency for the heavier witness disc. Which system provides better fidelity as a detonation performance diagnostic? We can compare the behavior of these two configurations with that from traditional larger scale results, both front-plate push experiments and cylinder tests.
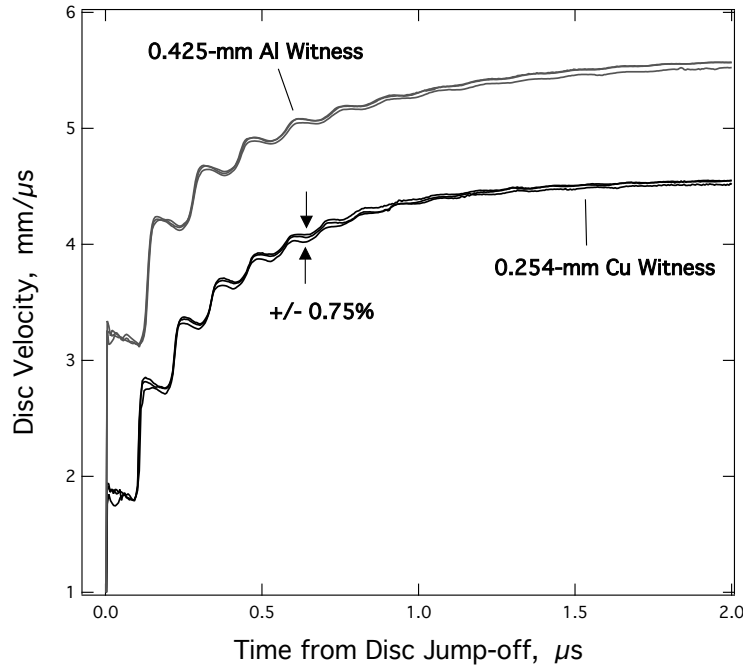

Figure 4: DAX data for the PETN-based explosive LX-16 (96.5/3.5 PETN/VCTFE). The plot shows three velocity-time traces for two separate configurations – using aluminum (top) and copper (bottom) witness discs. The disc velocity corresponds to the internal energy change in the expanding product gases, but the coupling efficiency to the plates varies with plate mass. Shot-to-shot repeatability is generally about 1% (standard deviation), but can be lower given sufficient care (see below in Discussion section).

Green & Lee's description [2-4] of PETN detonation performance can provide a baseline comparison for accurate assessments of detonation behavior using the DAX technique. They provide a Jones-Wilkins-Lee (JWL) EOS for pure PETN at a density of 1.762 g/cc [3]. That work sampled pure PETN without any binder, and the density was different than our densities. In addition, the geometry and diagnostics of those experiments were significantly different than the DAX geometry. Therefore, the most straightforward manner of comparing our results to those of Green & Lee is to derive our own JWL EOS that fits the DAX data, and then to make a direct comparison of the two JWL's. The Jones-Wilkins-Lee EOS is a rate-independent EOS that describes the pressure and energy of the product detonation gases as a function of their relative volume, $V = \rho_0/\rho$, which is equivalent to the density ratios of the initial and time-dependent product gases. The generalized JWL EOS can be written in closed form.

$$P = A\left(1 - \frac{\omega}{R_1 V}\right)e^{-R_1 V} + B\left(1 - \frac{\omega}{R_2 V}\right)e^{-R_2 V} + \frac{\omega E}{V} \tag{1}$$

This generalized relation has the following form on the adiabat (which we assume closely approximates the isentrope for a free gas expansion). The following equation fixes the adiabat the CJ point.

$$P_S = Ae^{-R_1 V_{CJ}} + Be^{-R_2 V_{CJ}} + \frac{C}{V_{CJ}^{\omega+1}} \tag{2}$$

The tangency condition at the CJ point in the P-V plane generates an additional relationship.

$$\left(\frac{dP}{dV}\right)_{CJ} = AR_1 e^{-R_1 V_{CJ}} + BR_2 e^{-R_2 V_{CJ}} + C\left(\frac{\omega+1}{V_{CJ}^{\omega+2}}\right) \tag{3}$$

Finally, a third equation can be derived for the energy of the expanding gases by effectively integrating the pressure (Eq. 1) over the volume, V.

$$E = \frac{A}{R_1} e^{-R_1 V_{CJ}} + \frac{B}{R_2} e^{-R_2 V_{CJ}} + \frac{C}{\omega V_{CJ}^{\omega}} \tag{4}$$

These three equations are simultaneously solved for A, B and C. The solution uses the CJ state as a boundary condition for the generalized solution:

$$\left(\frac{dP}{dV}\right)_{CJ} \equiv \frac{\Gamma P_{CJ}}{V_{CJ}} ; \quad P_S \equiv P_{CJ} ; \quad E \equiv E_0 + \frac{P_{CJ}(1-V_{CJ})}{2} \tag{5}$$

The experimental inputs include the initial density, detonation velocity, CJ pressure, and the chemical potential energy, E_0. This last value can be measured directly using detonation calorimetry, but is more easily estimated using a thermochemical code. The adjustable parameters for the JWL include R_1, R_2 and ω.

The explosive tested in this work has a lower average density (1.734 g/cc) than the Green & Lee JWL and contains 3.5% binder. These two differences must be accounted for in order to make a direct comparison of the DAX results with those from the traditional experimental configurations used in Green & Lee. We used the Cheetah thermochemical code [21] to adjust the Green & Lee JWL for PETN at 1.762 g/cc to a comparable LX-16 JWL at 1.734 g/cc. Each formulation was input into Cheetah and we compared the performance parameters, D_V, P_{CJ} and E_0, between the two cases. We then multiplied the Green & Lee PETN JWL values of ρ_0, D_V, P_{CJ} and E_0 by the ratio that Cheetah generated for each parameter for the two cases. The values for R_1, R_2 and ω were left untouched, and the system was self-consistently adjusted to obtain new values for A, B and C. Table 2 lists the JWL's for these two cases in columns 1 and 2, respectively.

This adjusted Green & Lee LX-16 JWL was set as our first trial EOS for modeling the new DAX data. We began with the aluminum disc data, and iteratively adjusted the P_{CJ}, R_1, R_2 and ω. A spreadsheet resolved the relevant JWL equations (2-4 above) and provided values for A, B, C and Γ (those variables required in the hydrocode input deck). Once a reasonable fit was made with the aluminum data, the model code was switched to the copper material and thickness, and the simulation was run once more without any change to the JWL. Column 3 shows the JWL that resulted from a fit to the entire set of DAX data. Adaptive mesh refinement was utilized in the hydrodynamic simulations. This technique uses coarse zoning in some areas, and finer zoning in those areas that require it for accuracy – such as at boundaries between different materials, and in the area around the witness plate. We have established through multiple simulations that the calculations were fully converged. In the converged case, the zoning in the witness disc was 810 zones per cm. Figure 5 shows the LX-16 DAX data along with the hydrodynamic simulations using the new Lorenz & Lee JWL from Table 2. While the match is not exact, it is still within ~1.5% in the region having the poorest fit. The excellent fit is especially encouraging when we recall that 33% more detonation energy coupled to the copper witness disc than the aluminum witness disc. Nonetheless, the fit in both cases using the same JWL is very good. We now must ask how close is this new Lorenz & Lee JWL - derived from the DAX technique, to the Green & Lee LX-16 JWL derived from more traditional, large-scale, experimental techniques?

8

Table 2: JWL's comparison of PETN and LX-16 for the purpose of validating the DAX technique. The Green & Lee PETN JWL (Column 1) was modified to an LX-16 JWL using the Cheetah thermochemical code (Column 2). This was then compared to a JWL fit to the DAX data in this report (Column 3).

| JWL Model	Green & Lee	Green & Lee*	Lorenz & Lee
Model ID	PETN	LX-16	LX-16
Mesh, z/cm	N/A	810	810
Density (g/cc)	1.762	1.734	1.734
Detonation Velocity (cm/μs)	0.8274	0.8024	0.81533
CJ Pressure (GPa)	31.5	29.55	30.0
R1	6	6	5.95
R2	2.6	2.6	2.65
A (GPa)	1029.47	907.76	958.18
B (GPa)	90.68	87.11	90.82
C (GPa)	3.726	3.494	3.420
w	0.57	0.570	0.555
Γ_{CJ}	2.8294	2.7781	2.8423
E_0, kJ/cm^3	10.80	10.18	10.18
Notes	1987 APS Shock Compression	* Adjusted from PETN EOS	DAX
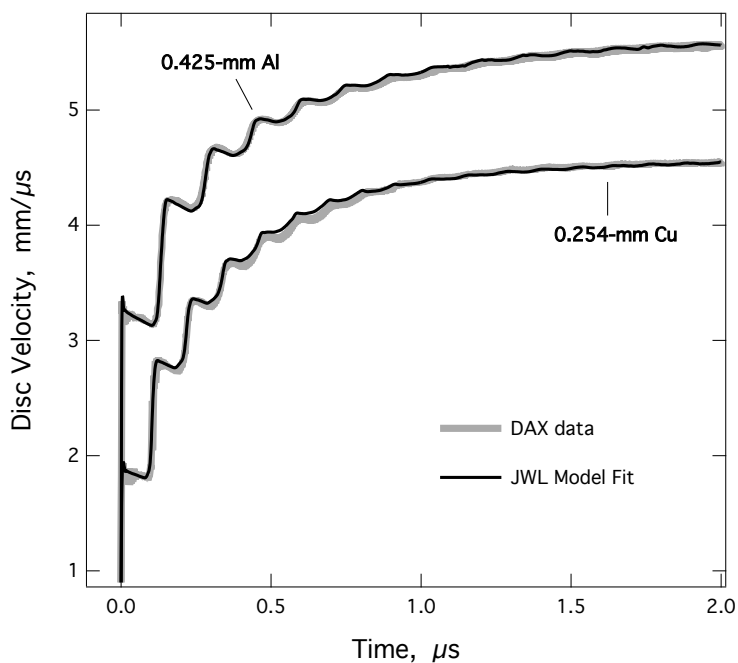
Figure 5: Modeling of the DAX data for LX-16. The two sets of DAX data (3 shots each) are depicted in light gray: data for 425μm thick aluminum discs (upper traces) and 250μm thick copper discs (lower traces). JWL model simulations are represented by the solid black lines. Note that the same JWL parameters (except the pellet density) were used for both sets of data.

Figure 6 compares the Green & Lee and Lorenz & Lee JWL's within the DAX simulation space. We ask, how do the DAX simulations using the two JWL's compare to one another? The plot shows the percent difference between the new Lorenz & Lee JWL and the Green & Lee JWL as a function of flight time for the DAX witness disc. A positive value indicates a higher velocity (energy) for the new JWL. The lighter traces are highly oscillatory because of small phase differences in the reverberations of the two JWL simulations. For clarity, we included smoothed profiles of the percent difference traces as solid lines. Across most of the measured time domain, the two models generate DAX simulations that are within ±0.5% of each other in velocity, or ±1% in energy.
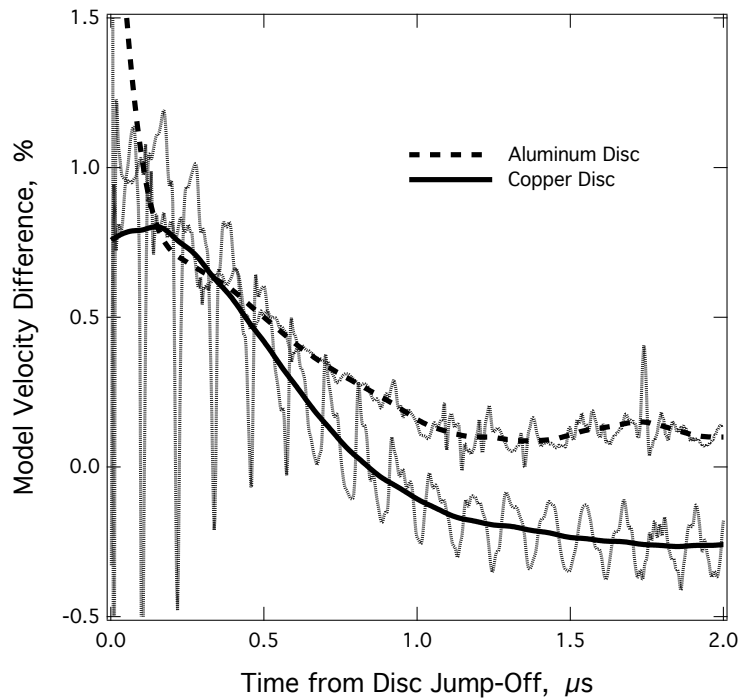

Figure 6: Comparison of the Lorenz & Lee LX-16 JWL with the Green & Lee LX-16 JWL (adapted from the Green & Lee PETN JWL) within the DAX simulation space. Positive values represent higher disc velocities for the Lorenz & Lee model. The oscillatory records have been smoothed to aid the reader. For a comparison of the energy differences, double the values on the y-axis.

As a final comparison of the two models, we present in Figure 7 the calculated energy of each model as a function of the relative volume within an isentropic (adiabatic) expansion. Comparisons were made analytically (by solving the Eq. 2-4 above) using the JWL parameters to derive ideal isentropic expansion energies. These energies are in close agreement from maximum compression to relative expansion volumes of ~3. At that point the energies diverge slightly. The DAX model predicts ~1% higher energy than the Green & Lee model at mid-to-large expansion volumes. The DAX method's geometry should limit the accuracy of the technique to expansion volumes less than ~3, which is when the release waves from the sidewalls are expected to have a significant affect on the trajectory of the witness disc. Nonetheless, the EOS extracted from this limited expansion regime matches the Green & Lee JWL. That EOS used data from both larger font plate push experiments, as well as large scale cylinder tests having measurable expansion volumes of 8-10. Besides the scale of the experiments, the DAX method differs from the traditional techniques in two significant ways. First, even though the DAX samples a smaller range of relative product gas volumes than a traditional cylinder test, it is much more sensitive to the CJ

region of the detonation. Normally, analysis of cylinder test data relies on the wall energies at relative volumes above 2-3. The CJ pressure becomes a floating parameter in the overall fit to the volume-dependent wall energy. In this regard, the DAX method complements the cylinder test method. Second, the DAX detonics establish steady state flow before the detonation front begins to push on the witness disc. In contrast, early plate-push experiments used by Green & Lee to establish the density-dependent CJ pressure of PETN (similar to those by Deal [11] and Duff & Houston [12]) established centered flow detonation. That type of geometry requires a clear understanding of the initial boundary conditions set up by the detonator and booster portions of the shot assembly. For that reason, the modeling task for extracting an accurate CJ pressure in the DAX geometry is more straightforward.

In the next section, we will discuss two methods for directly extracting the CJ pressure from the velocity-time data near the jump-off region. This can be an important tool for quickly estimating this critical performance parameter – especially if the experimentalist lacks the resources to carry out hydrodynamic simulations.
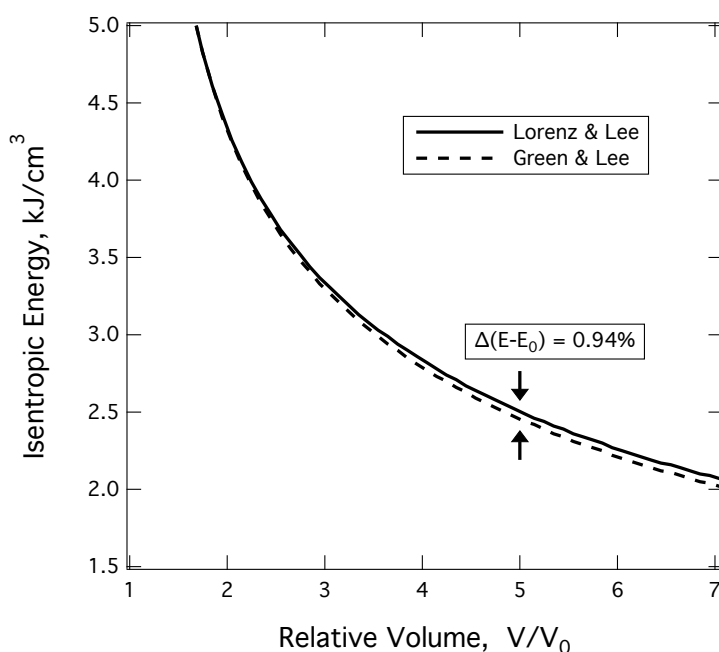

Figure 7: LX-16 model isentropes for the JWL's extracted from DAX (this work, solid line) and traditional cylinder tests (Green & Lee, dashed line). The model energies are within 1% out to relative volumes beyond 7. This is encouraging since the DAX geometry is expected to encounter strong side-release waves at relative volumes of ~3.

EXTRACTING CJ PRESSURES FROM THE VELOCITY-TIME RECORDS

There are two basic methods we use to estimate the CJ pressure from the velocity-time records. Both of these methods assume that the reaction zone thickness is less than the thickness of the witness disc. For a PETN based explosive formulation like LX-16, this is expected to be the case. In the analyses below, we begin with the assumption that the von Neumann pressure spike attenuates well before the shock front reaches the rear face of the witness-disc.

Method 1: Linear extraction of the pullback region

This method is effectively the same method used by Deal [11] and later Davis and Venable [13]. Both groups used the technique to measure the detonation pressure of Composition-B. The technique maps the shape of the rarefaction (Taylor) wave in the explosive as it proceeds through increasingly thinner witness plates. The wave profile is then extended to a zero-thickness condition to obtain the necessary Hugoniot information in the metal to determine the pressure in the explosive using an impedance match calculation across the metal-explosive interface. Deal and Davis used timing pins to obtain shock velocities as a function of witness disc thickness. Using the standard Hugoniot relation, the shock velocity at the metal-explosive interface (zero witness disc thickness) can then be used to determine the particle velocity in the metal.

$$U_P^* = \frac{U_M^* - C_0}{s}$$ (5)

The bulk sound speed, C_0, and s are the experimentally determined Hugoniot values for the metal disc, and, U_P^* and U_M^* are the particle velocity and shock velocity at zero thickness, respectively. This technique must rely on a series of separate detonation experiments. However, the PDV technique provides a continuous time record of the plate acceleration, and this allows us to make a CJ-pressure determination from a single detonation experiment.

The PDV measures the free-surface velocity of the accelerating thin witness disc under the imposed load of the detonation wave. The temporal shape of the detonation profile leads to a reverberating wave in the witness disc (see Figure 3 above). These reverberations are caused by the back-and-forth passage of shock waves in the disc. The times between successive reverberations are round-trip times for a forward-going and reflected shock in the witness disc. The slowly decreasing velocity after each abrupt velocity jump reflects the shape of the shock wave in the metal disc, which itself is a reflection of the shape of the detonation wave in the explosive. The first pullback region after the initial jump depicts the back-and-forth wave action after the wave has made a single transit in the witness disc. By tracing the profile of this first pullback region backwards in time by exactly half of a round trip time, we can estimate the pressure at the head of the shock wave at the zero-thickness condition. An extrapolation in time of the velocity in the first pullback gives a free-surface velocity for a witness disc having zero thickness. (Note, that this assumes a steady shock velocity through the plate, which is an approximation. We correct for this in the next section.) The free-surface velocity at a jump state is twice the particle velocity in the metal at that point in thickness.

$$U_P^* = U_{FS}^*/2$$ (6)

U_{FS}^* is the extrapolated value from the linear fit to the jump-off region. Figure 8 shows the extrapolated fits of the pullback regions for the two LX-16 DAX datasets. Each figure shows the compilation of velocity-time points for two or three shots, and a linear fit to a point in time that is half the round trip time before the jump-off time. (The record for shot TLX-XII-048 [left hand plot, dashed line] was not included in the linear fit because the record in the jump off region had considerably more noise than the other two records, and we considered it to be spurious in this region.)

The zero-thickness particle velocity, U_P^*, can be combined with the measured detonation velocity, D_V, and explosive density, ρ_0, to determine the CJ pressure in the explosive [11].

$$P_{CJ} = (U_P^*/2) [\rho_0 D_V + (\rho_M U_M)]$$ (7)

The shock velocity in the metal, U_M, is also a function of the extrapolated particle velocity.

$$U_M = C_0 + sU_P* \tag{8}$$

So, it is necessary to have accurate Hugoniot data for the witness disc materials. We relied on the Steinberg's Hugoniot values for Aluminum-1100 and soft (OFHC) copper [22].

Aluminum-1100: ρ_M = 2.707 g/cc, C_0 = 5.386 mm/µs, s = 1.339

Soft (OFHC) Copper: ρ_M = 8.930 g/cc, C_0 = 3.940 mm/µs, s = 1.489

This methodology gives CJ pressure values of 28.46 ± 0.31 GPa for the DAX shots using aluminum witness discs, and 31.03 ± 0.57 GPa for the DAX shots using copper witness discs. This discrepancy can be explained by viewing the method pictorially in the P-U_P space.
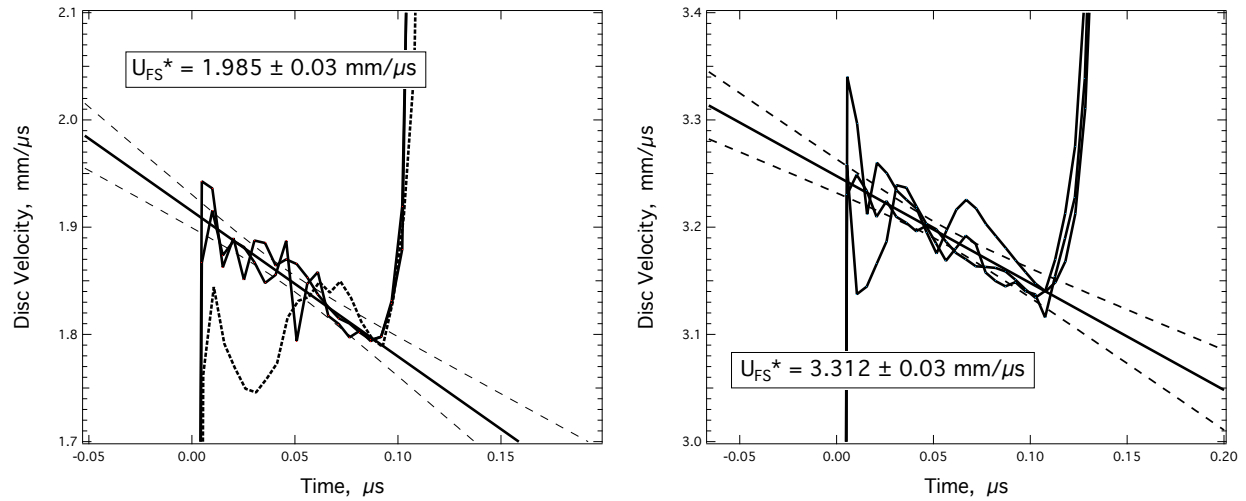

Figure 8: Extrapolations of the measured disc velocities in the jump-off region of the velocity-time data. The velocities are extrapolated beyond the jump-off time to a point that is earlier by half the round-trip time of the shocks in the plate. These round trip times are the times between steps in the velocity-time trace. This represents the approximate time that the detonation wave reached the explosive-metal interface. The particle velocity in the metal witness disc at the metal-explosive interface is half the value of this extrapolated velocity.

Figure 9 shows this impedance matching technique in graphical form. The P-U_P equations-of-state for the metal disc and the explosive are crossed to determine a common solution for the measured particle velocity at the metal-explosive interface. For the metal, we use their respective Hugoniots. For the explosive we approximate its product-gas EOS with the Rayleigh line, which we can determine form the measured density and detonation velocity. This approximation is corrected in the section that follows. The solutions for the aluminum and copper cases differ by about 2.57GPa, which gives us an average CJ pressure for this technique of 29.75 GPa ± 4%. We will see below that this average value turns out to be very close to the value arrived at by hydrodynamic simulations of the velocity-time profiles. However, the spread in the two values is indicative of the hazards of using the various simplifications stated above – that is, an assumption of a steady shock velocity in the metal witness disc, and the use of the Rayleigh line for the product-gas EOS. Given the discrepancy of the solutions for the two different witness disc materials, one may ask whether the average value is taken to be the correct value for the CJ pressure.

A closer look at the model simulations can demonstrate the confidence we place in the average value of the CJ pressure we made from the analysis above. Figure 10 shows an expanded view of the velocity-time data in the jump-off region (copper case). We also show the final model fit of the data (heavy green line). We ran several more simulations using higher and lower CJ pressures to determine how far the "fits" diverged from the original data. These alternate JWL's remained self-consistent: the values of ρ_0, D_V, R1, R2, ω and E_0 remained. But A, B and C floated with the change in P_{CJ}. It is clear from the plot that the data falls within 1-2% of the simulated CJ pressure. The model simulations leads us to believe that the 30.00 GPa CJ pressure we estimate from those simulations is good to within 2%. Therefore, the spread in the estimated CJ pressure values from the linear extraction method should be indicative of the two approximations we made in the impedance matching analysis, and does not lie in the data or the method we use for extracting the CJ pressure. The next section will discuss a more rigorous method of extracting the CJ pressure from the DAX velocity-time profiles.
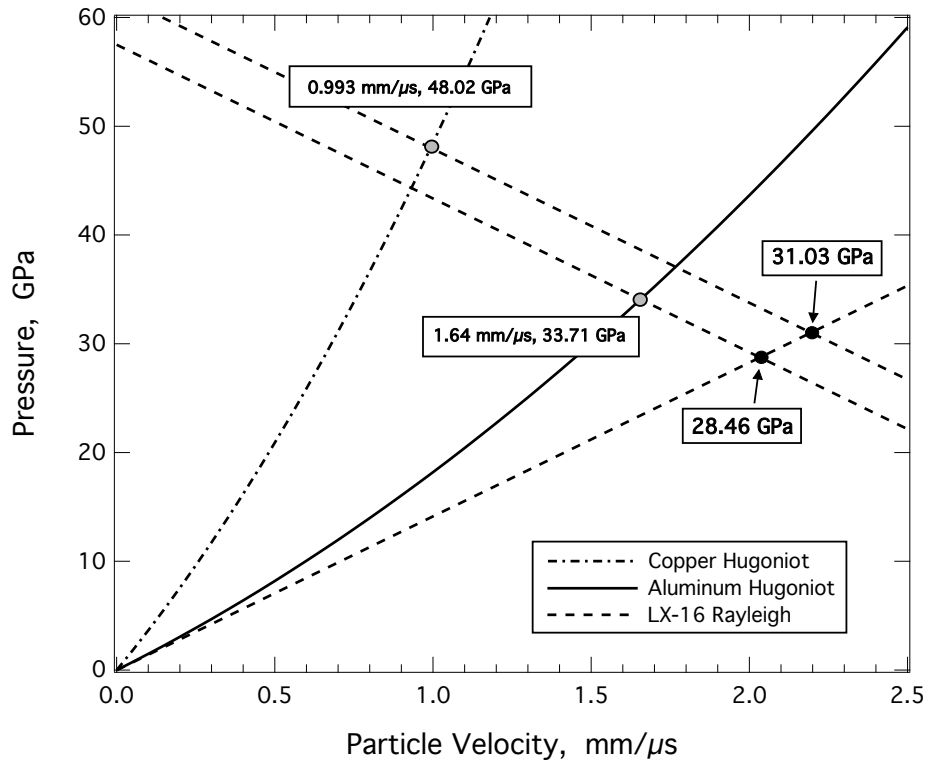

Figure 9: Graphical method for extracting the CJ pressure using the Rayleigh line for the product gas EOS. The technique uses the particle velocity at the metal-explosive interface (U_P*) as input for impedance matching across the metal-explosive interface. The metal Hugoniots are shown as dash-dot (Cu) and solid (Al) lines. The linearly extracted U_P*, P_M* are shown as gray dots on the metal Hugoniots. The reflected Rayleigh line (dashed) is then placed through these points, and the CJ point is designated as the intersection of each Raleigh and Reflected-Rayleigh pair (solid dots).
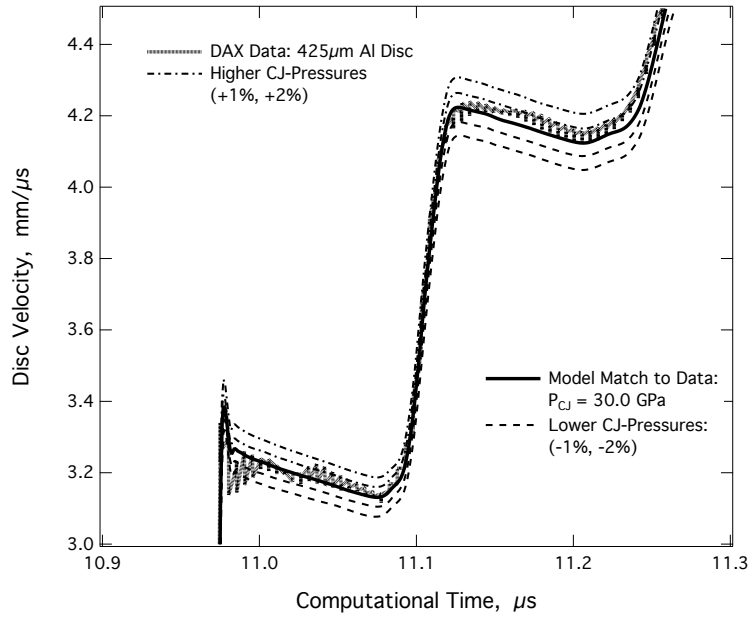
Figure 10: JWL modeling of front jump-off region from LX-16 DAX data. The sensitivity to CJ pressure is high. The model simulation diverges from the data with a variance in the model CJ pressure of not more than 1-2%. This model sensitivity suggests that the DAX data can generate reliable CJ pressure determinations of better than ~2%.

Method 2: Corrections for Shock Attenuation and Product-Gas EOS

We have stated above that the JWL fit to the DAX data is very sensitive to the input CJ pressure. One could also say that the DAX data provides a sensitive measure of the CJ pressure – a critical performance metric for all explosives. The density and detonation velocity are determined in a straightforward manner. But CJ pressure has always been difficult to determine, because the end of the reaction zone is not always obvious even if we can measure the pressure of the detonation with high precision. One solution is to simply estimate the CJ pressure from the density and detonation velocity:

$$P_{CJ} \approx \tfrac{1}{4}\, \rho_0\, D_V^2 \tag{9}$$

This method may get one in the ballpark, but is not very accurate. For this work, Eq. 9 leads to a CJ pressure of 28.82 GPa – about 3% lower than the average value found from the linear extraction method above. That analysis made an approximation in the impedance matching technique. This approximation used the Rayleigh line as an approximation of the detonation product Hugoniot:

$$P_{GAS} \approx (\rho_0\, D_V)\, U_P \tag{10}$$

15

A more correct analysis assumes that the shock wave in the metal witness disc decays exponentially, and the detonation product EOS is not a linear relation in the P-U_P plane – as is the Rayleigh line described by Eq. 6.2. The behavior of the shock attenuation in a copper plate at the end of our DAX assembly is simulated in Figure 6-7 below. We used the LX-16 EOS that was fit to the DAX data to depict disc velocity results for an array of copper disc thicknesses – in order to determine what the particle velocity would be under the detonation-induced shock at the copper / LX-16 interface. The plot simulates disc thicknesses from 50µm to 1000µm. It is clear that the jump-off velocity decreases in a non-linear fashion, so a linear extrapolation from the pullback region data using a 250µm disc will ***under-predict*** the particle velocity at zero-thickness. The decay can be fit to an exponential function, as seen by the right-hand plot in Figure 11.
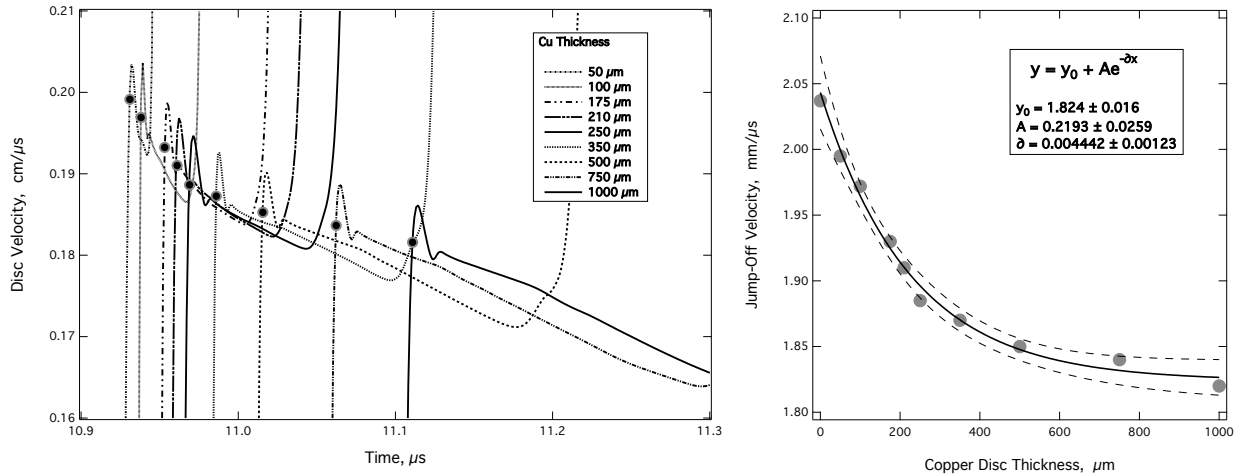

Figure 11: JWL modeling of the decay of the detonation-induced shock wave in the copper witness disc. Because the decay is non-linear, a linear extrapolation of the DAX data's pullback region leads to an under-prediction of the CJ pressure. The error in CJ pressure is small, but simple corrections can still be utilized to reduce this error.

The extrapolation to zero-thickness gives a free surface value of 1.824 + 0.2193 = 2.043 mm/µs, which corresponds to a particle velocity in the copper at the interface of 1.022 mm/µs. This can be compared to the linear extrapolation value of 0.9925 mm/µs. This difference leads to a 10-kbar difference in CJ pressure after an impedance matching analysis. We are in the process of confirming the functional form of the decay for different initial jump-offs (for different explosives) and different initial plate thicknesses. This will allow a general correction factor for any reading of the jump-off value that is independent of the explosive's performance, or the disc thickness.

A second correction to the CJ-pressure analysis is affects the manner in which we represent the product gas Hugoniot. Instead of using the Rayleigh line for the product EOS, it would be best to use the actual EOS for the explosive formulation that we are testing. However, that is not always available – especially if you do not have the modeling resources and simply want to extract the most important performance parameters from the DAX data [such as detonation velocity, CJ pressure and E_3 energy]. Cooper has developed a generalized EOS [23] that can be iteratively fit to the impedance conditions of the DAX experiment. Cooper's general expression in the P-U_P space is applicable for a wide range of product EOS's, and can be expressed in a reduced form in terms of the explosive's CJ state [P_{CJ}, U_{CJ}].

$$\frac{P}{P_{CJ}} = 2.412 - 1.7315 \left(\frac{U_P}{U_P^{CJ}} \right) + 0.3195 \left(\frac{U_P}{U_P^{CJ}} \right)^2 \tag{11}$$

16

Using the equation above, one can substitute trial values for the P_{CJ}, U_{CJ} pair [this assumes the relation $P_{CJ} = \rho_0 D_V U_{CJ}$ holds for the CJ state] such that the function passes through the experimental data points P^*, U_P^*. The asterisk indicates the extracted particle velocity and pressure in the metal disc at the HE-metal interface. Eq. 9 can be solved analytically to find the CJ pressure. The product gas Hugoniot must pass through the metal witness disc Hugoniot at the impedance matching condition, that is, at the P^*, U_P^* point on the metal line. Therefore, we can substitute P^* for P, and U_P^* for U_P in Eq. 11. Then one needs to express P_{CJ} in terms of the particle velocity.

$$P_{CJ} = \rho_0 U_P^{CJ}\left(C_0 + sU_P^{CJ}\right) \tag{12}$$

Eq. 11 and 12 are rearranged and form a quadratic that can easily be solved via the Quadratic Equation, and taking the positive root.

$$U_P^{CJ} = \frac{d + \sqrt{d^2 - 4ac\left(U_P^*\right)^2}}{2a}, \ where \ \ a = 2.412, b = 1.7315, c = 0.3195 \tag{13}$$

$$and \ \ d = \frac{P^*}{\rho_0 D_V} + b(U_P^*)$$

Figure 12 should help the reader by depicting this new analysis in graphical form. The P_M^*, U_P^* pairs for the copper witness disc and aluminum witness disc experiments are 1.022 mm/μs, 49.82 GPa and 1.773 mm/μs, 36.85 GPa, respectively. The interface particle velocity, U_P^*, in the copper plate is noted on the metal Hugoniot lines by red (Cu) and blue (Al) dots.
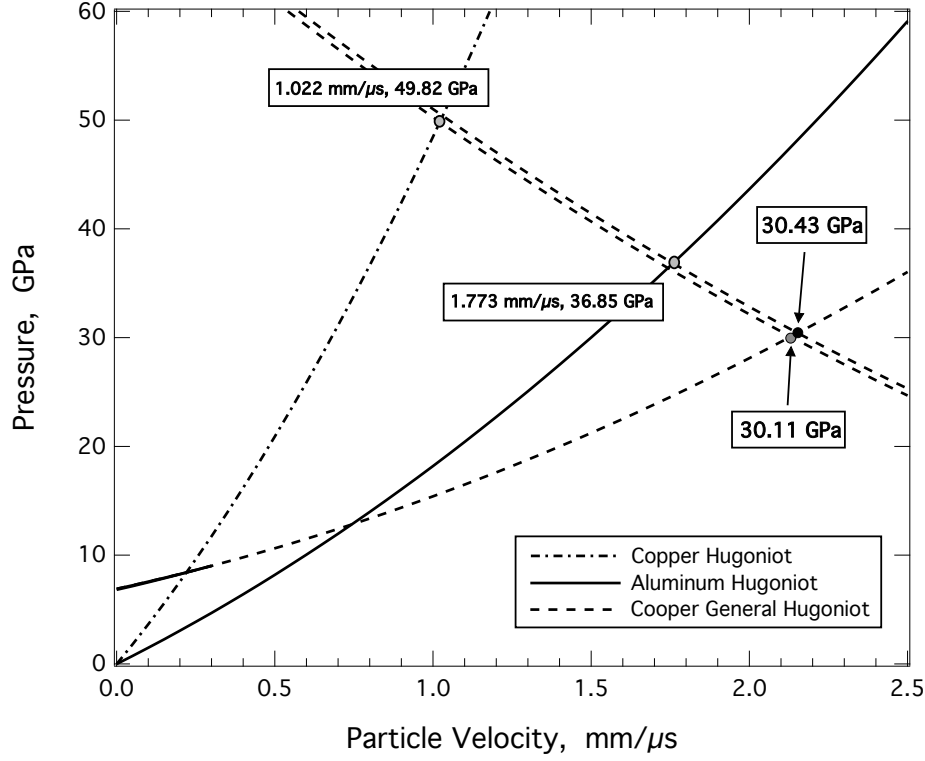
Figure 12: Impedance matching relations for DAX using a more realistic product-state Hugoniot and a better estimate of the particle velocity at the metal-explosive interface. This analysis uses an exponential decay to describe the shock attenuation in the metal witness disc, which slightly alters the estimate of the particle velocity at the metal-HE interface (compare to Figure 9). The analysis also uses a more accurate Cooper product-gas EOS [22] that is determined by an iterative process of fitting a generalized EOS to the CJ impedance matching condition of each configuration.

These adjusted particle velocities, U_P*, in this plot are slightly larger than those derived from a linear extrapolation of the DAX pullback data (see Figure 9). The generalized Cooper product EOS is solved for these P_M*, U_P* pairs by either graphical analysis or algebraic solution. We show the graphical analysis for clarity in Figure 12. One inputs a trial CJ condition – U_{CJ}, P_{CJ}, assuming that

$$P_{CJ} = \rho_0 D_V U_{CJ} \qquad (12)$$

The resulting $P(U_P)$ solution is placed onto the plot. Does it pass through the desired P_M*, U_P*? If not, adjust the U_{CJ}, P_{CJ} input until a satisfactory solution is obtained. For clarity (and as a comparison to the impedance matching plot from Figure 9) we also show the Cooper solutions reflected about the CJ state. The more realistic product EOS's, along with the adjusted particle velocities in the witness discs, lead to CJ pressure values from the copper and aluminum systems that are in close agreement with one another, as well as the hydrodynamic simulations. The results for the two different CJ-pressure analyses are shown in Table 3, and compared to the values derived from the hydrodynamic simulations using a JWL EOS and programmed burn.

18

Table 3: Values for LX-16 CJ pressure extracted directly from data, and via hydrodynamic modeling. "Method 1" refers to an approximation of extracting the metal particle velocity (at the HE-metal interface) using a linear extrapolation of the pullback region of the DAX data. "Method 2" refers to adding a correction to the linear decay of the shock pressure in the metal for an exponential decay function. The uncertainties for the model simulations are set at ±1.5% based on what is shown in Figure 10.

Configuration	U_P*, Method 1 (mm/µs)	U_P*, Method 2 (mm/µs)	P_{CJ}, Method 1 (GPa)	P_{CJ}, Method 2 (GPa)
0.425-mm Aluminum Disc	1.640 ± 0.030	1.773 ± 0.061	28.46 ± 0.31	30.43 ± 0.61
0.254-mm Copper Disc	0.993 ± 0.030	1.022 ± 0.030	31.03 ± 0.57	30.11 ± 0.53
JWL Model Simulation	-	-	30.00 ± 0.45	30.00 ± 0.45

DISCUSSION SECTION

The DAX technique began as an effort to design a low-cost, characterization tool that could be used in the early stages of an explosive R&D program to assess the performance of a new explosive or explosive formulation. It had to address the common performance metrics, use a relatively small amount of sample material, and be easy to assemble and field. The choices for the current DAX design were influenced by several factors. First, the standard cylinder tests are inherently expensive due to the required machining tolerances for copper tubes. The wall thickness must be maintained to very high precision over a long bore. By comparison, the DAX uses commercial grade rolled sheet stock for its witness discs. The discs are laser cut, but could easily be punched out using a die tool. Second, the clear plastic tubing in the DAX allows for easier assembly (no blind gaps inside the tube) and the low impedance of the plastic makes the detonics insensitive to gaps between the sample and the walls. Third, the temporal resolution and dynamic range in modern PDV systems allows the use of thin witness discs in a front plate push design. This makes the experiment much more sensitive to the CJ state than cylinder test geometries. Finally, from a geometry perspective, we chose to forego planarity across the detonation front, and focused on establishing steady detonation in the current configuration. That choice results in 2D effects, but they are well behaved and can be readily modeled. The trade-off establishes steady state detonation in the explosive sample that eliminates any sensitivity to initial boundary conditions near the booster/detonator.

There are a few issues with the DAX design that are not present in traditional cylinder test geometries. These include: (1) a lower coupling value of the available detonation energy to the energy of the witness disc, (2) a reduced range of relative product gas volumes sampled over the duration of the experiment, and (3) a lack of strict correspondence between the witness disc displacement and the relative volume of the detonation gases behind the plate. The first issue resolves itself with sufficient precision in the plate velocity diagnostic. We have demonstrated that we can track witness disc energy to better than 1%, which indicates that we can resolve the difference in performance between two explosives to that level – as long as the coupling efficiency is the same for the two explosives. The coupling efficiency depends to first order on the relative mass of explosive to witness disc, so differences in density would lead to slightly different coupling efficiencies. However, the coupling function changes slowly (as a function of the ratio of explosive density to witness disc density) in the regime we are working [18]. Though this issue would also be present in cylinder tests, we do not believe that it is significantly affecting the fidelity of our current measurements. The second and third issues arise because of the 2D geometry of our assembly. Unlike the cylinder test, in which the expansion can be successfully analyzed as radial flow, in the DAX test both the radial and the axial flow are important. The loss of energy in the lateral dimension limits the energy transferred to the witness disc at the end of the charge at longer times (or larger gas volumes). These flow dynamics effectively limit the validity of the data to a product gas expansion volume of ~3. By comparison, cylinder test measurements acquire reliable wall-velocity data out to relative volumes beyond 10. This disparity in sampling efficiency is mitigated by the fact that more than 70% of the available detonation energy has been released at a relative volume of 3. A more challenging issue is the poor

correlation between witness disc displacement and product gas volume. The cylinder test wall energy at any specified wall displacement is known directly from the wall velocity, and this is then correlated directly to the energy of gas expansion at a specific volume on the adiabat. Thus, the cylinder test data correlates detonation energy with gas volume in a predictable and direct fashion. These concerns were successfully resolved for the DAX technique by carrying out multiple 2D hydrodynamic simulations of the disc velocity histories. The simulations can account for lateral energy losses in the DAX geometry. And we see here that the LX-16 JWL derived from the DAX data agreed (to within 1%) with the JWL from cylinder tests, where the JWL was fit to gas volumes as large as 10. Additional work on less ideal materials may show that the DAX technique is more limited - in some subtle fashion - than our current estimation.

The sensitivity to the CJ region may prove to be one of the more appreciated aspects of this new test. Measurements for P_{CJ} have traditionally been carried out using large diameter charges initiated by plane wave boosters in order to produce nearly flat detonation front profiles, and this arrangement can simplify analysis. However, those experiments [11-13] were susceptible to influences from the detonator/booster assembly. In fact, they were described as centered flow, and not steady detonation. Therefore, the release wave behind the detonation front (also called the Taylor wave) must be well understood in order to accurately determine the CJ pressure. But a bigger difference is in diagnostics. The PDV technique allows us to make a continuous velocity-time record of the interaction of the detonation wave with the witness plate. The resulting wave reverberations contain the essential information that is needed to extract the pressure at the front of the detonation. In the ZND detonation model [24], the von Neumann pressure spike is relatively narrow, and attenuates much more rapidly in an inert medium than the following Taylor wave. This dynamic made it possible for experiments using non-continuous diagnostics to determine the CJ pressure – but also required a series of experiments using successively thicker witness plates. But DAX tracks the falling pressure continuously and therefore the only restriction is that the witness disc be thick enough to attenuate the von Neumann spike before the pressure wave reaches the back surface.

It is fair to ask whether the DAX test can be applied successfully to explosives that exhibit non-ideal behavior. For less ideal material having thicker reaction zones you could use a thicker plate. This is easily done by dimensionally scaling the DAX geometry. The plate thickness can be simply doubled, or the whole geometry can be scaled by 2x. The cost increase is marginal. The downside is the need for more sample material. This issue is not easily avoided, but can be mitigated. A non-ideal explosive can be successfully tested using DAX as long as a steady detonation is achieved. That is, the charge diameter must be greater than the inherent failure diameter of the explosive. Given this limitation, the plate dynamics can be evaluated using a rate-dependent equation-of-state. The CJ condition in this case is convolved with the von Neumann spike and the modeling analysis is more challenging. The experimentalist can either run additional DAX experiments at successively larger dimensional scales, or execute an independent experiment that can provide information about the detonation kinetics. It should even be possible to run multiple experiments at the same scale but with different witness disc thicknesses.

We view the success of this work as crucial to our plan to apply DAX technology to new explosives including many which are less 'ideal" in performance than the PETN based explosive in this work. The EOS extracted from this new DAX technique for LX-16 is a close match to a comparable Green & Lee EOS developed from the large-scale experiments. The EOS developed in the Green & Lee work also required a choice for P_{CJ} consistent with our measured P_{CJ}. We are able to demonstrate that the EOS derived from the DAX measurements closely agrees with the EOS for an equivalent PETN high explosive based on cylinder test results. This LX-16 EOS serves as proof of the new DAX capability and as a validation against an accepted detonation performance standard.

CONCLUSIONS

Detonation performance of a well-known, PETN-based explosive – LX-16, was used to validate a new small-scale performance test. This Disc Acceleration eXperiment (DAX) uses less than 20 grams of sample explosive in a simple assembly to measure three critical performance parameters; detonation velocity, CJ pressure and the expansion energy at a relative volume of ~3. Detonation velocities are extracted from position-time data generate by piezoelectric pins placed at precision points along the side

of the assembly. The CJ pressure and expansion dynamics are tracked via a thin metal witness disc at the end of the sample charge using Photonic Doppler Velocimetry (PDV). This technique [15] is highly modular and relies on commercial components. The architecture of the technique allows us to perform four experiments simultaneously – greatly saving experimental costs. The PDV data is amenable to hydrodynamic modeling and can therefore be used to generate an equation-of-state (EOS), which can then be used for further design purposes. The availability of an accurate EOS for design trials at the early stages of a new explosive's development has been much desired in the HE R&D community.

The DAX technique has been demonstrated here using two different witness discs – 0.254-mm thick copper and 0.425-mm thick aluminum. Disc velocity was repeatable to better than 1% in each case. Model simulations of the data using a Jones-Wilkins-Lee EOS showed excellent agreement with a JWL based on the well-established Green & Lee PETN JWL [2-4]. The model agreement is maintained across a large region of the expansion space – well beyond the design space for this small-scale device. We show two different analyses of the jump-off region of the PDV data that can provide highly accurate determinations of the CJ pressure, provided the witness disc is thicker than the explosive's reaction zone. Using rate-dependent modeling, this requirement can be softened.

The new DAX technique takes advantage of the capabilities of PDV to make a new detonation tool available to the R&D community that matches the precision of the traditional cylinder test, but drives the costs down as much as an order of magnitude.

ACKNOWLEDGEMENTS

REFERENCES

1. D. L. Ornellas, "Calorimetric determinations of the heat and products of detonation for explosives: October 1961 to April 1982", UCRL-52821, Lawrence Livermore National Laboratory, Livermore, CA (1982).

2. H. C. Hornig, E. L. Lee, M. Finger and J. E. Kurrle, "Equation of State of Detonation Products", 5th International Symposium on Detonation, Pasadena, CA, August 18-21, 1970, pp. 503-511 (1970).

3. L. Green, E. L. Lee, D. Breithaupt and J. Walton, " The Equation of State of PETN Detonation Products", Proceedings of the 1987 APS Topical Group on Shock Compression of Condensed Matter, pp. 507-510 (1988).

4. L. G. Green and E. L. Lee, "Detonation Pressure Measurements on PETN", Thirteenth Symposium on Detonation, Norfolk, VA, July 23-28, 2006, pp. 1134 (2006).

5. P. W. Cooper and S. R. Kurowski, Introduction to the Technology of Explosives, pp. 72-82, Wiley-VCH, New York (1996).

6. M. L. Wilkins, "The equation-of-state of PBX-9404 and LX-04-01", Lawrence Livermore National Laboratory, Livermore, CA, report UCRL-7797, (1964).

7. E. L. Lee, "Adiabatic expansion of detonation products", UCRL-50422, Lawrence Livermore National Laboratory (1968).

8. E. L. Lee, H. C. Hornig, and J. W. Kury, "Adiabatic Expansion of High Explosive Detonation Products," Lawrence Livermore National Laboratory, Livermore, CA, report UCRL 50422, (1968).

9. J. W. Kury, H. C. Hornig, E. L. Lee, J. L. McDonnel, D. L. Ornellas, M. Finger, F. M. Strange, M. L. Wilkins, "Metal Acceleration by Chemical Explosives," Proceedings Fourth Symposium (International) on Detonation, White Oak, MD, October 12-15, 1965, pp. 3-13 (1965).

10. P. C. Souers, personal communication (2014).

11. W. E. Deal, Jr., "The Measurement of Chapman-Jouguet Pressure for Explosives", Second ONR Symposium on Detonation, Washington, D. C., February 9-11, 1955, pp. 209-224 (1955).

12. R. E. Duff, and E. Houston, "Measurement of the Chapman Jouguet Pressure and Reaction Zone Length in a Detonating High Explosive," Second ONR Symposium on Detonation, Washington, D. C., February 9-11, 1955, pp. 225-239 (1955).

13. W.C. Davis and D. Venable, "Pressure Measurements for Composition B-3", Proceedings from the 5th Intl. Detonation Symposium, pp. 13-22, Office of Naval Research ACR-184, Pasadena, CA (1970).

14. L. G. Green, E. L. Lee, A. Mitchell and C. M. Tarver, "The Supercompression of LX-07, LX-17, PBX 9404 and RX-26-AF, and the Equation of State of the Detonation Products", 8th International Detonation Symposium, pp. 587-595 (1986).

15. O. T. Strand, D. R. Goosman, C. Martinez, T. L. Whitworth and W. W. Kuhlow, "Compact System for High-speed Velocimetry using Heterodyne Techniques", *Rev. Sci. Instrum.* **77**, 083108 (2006).

16. Model CA-1135, Manufactured by Dynasen, Inc., Goleta, CA.

17. C. M. Tarver and C. M. May, "Short Pulse Shock Initiation Experiments and Modeling on LX-16, LX-10 and Ultrafine TATB", 14th International Detonation Symposium, pp. 648-663 (2010).

18. A.K. Aziz, H. Hurwitz and H. M. Sternberg, "Energy transfer to a rigid piston under detonation loading", Physics of Fluids 4(3), 380-384 (1961).

19. R.W. Gurney, "The initial velocities of fragments from bombs, shells and grenades", B.R.L. Report 405 (1943).

20. R. Karp and P.C. Chou, in *Dynamic Response of Materials to Intense Impulse Loading*, Eds. P.C. Chou and A. P. Hopkins, Air Force Materials Laboratory, WPAFB, Dayton, Ohio (1972). Taken from p. 233 of M. Meyers, *Dynamic Behavior of Materials*, Wiley & Sons, New York (1994).

21. CHEETAH Performance Code, v. 6.0, Rev. 1794, LLNL-CODE-434431.

22. D. J. Steinberg, "Equation of State and Strength Properties of Selected Materials", Lawrence Livermore Laboratory, Livermore, CA, LLNL Report UCRL-MA-106439 (1996).

23. P. L. Cooper, Explosives Engineering, Wiley-VCH, New York, p. 267 (1996).

24. Ia. B. Zeldovich and A. S. Kompaneets, Theory of Detonation, Academic Press, New York, pp. 68-84 (1960).